Journal of Applied Phycology
https://doi.org/10.1007/s10811-026-03815-x

RESEARCH

Light limitation reduces proportion of the released methane to assimilated carbon and nitrogen in the N_2-fixing cyanobacterium *Trichodesmium*

Chuze Zou[1] · **Kunshan Gao**[1,2]

Received: 5 November 2025 / Revised: 5 February 2026 / Accepted: 9 February 2026

Abstract
Trichodesmium, a nitrogen-fixing cyanobacterium, has recently been shown to release methane through utilization of the organic phosphorus methylphosphonate (MPn), which is commonly found in surface oceans. We demonstrated previously that methane production (MP) increased with rising temperatures and was positively correlated with assimilations of carbon and nitrogen under optimal light conditions. Here, we show that when grown under light-limitation, elevated temperatures within a range of 23 °C to 31 °C reduced growth by 67% and MP by 91%, with altered relationship of MP to assimilations of C, N and P. This indicates that light-limitation disrupted the synergy of MP with the C/N/P assimilations, highlighting that photosynthetic energy supply affects methane production to differential extents with increasing temperatures. Our results imply that *Trichodesmium* in deeper waters or exposed to low light conditions produces much less methane even under ocean warming scenarios.

Keywords Cyanobacteria · Light · Methane production · Nitrogen fixation · Photosynthesis · Temperature · *Trichodesmium*

Introduction

Methane (CH_4), a potent greenhouse gas, has a global warming potential about 80 times greater than that of carbon dioxide over a 20-year period, despite its relatively short atmospheric lifetime (~ 10 years) (IPCC 2013; Saunois et al. 2020). Historically, methane production was attributed to anaerobic methanogenesis performed by archaea (Karl and Tilbrook 1994). However, the widespread observations of methane supersaturation in oxygenated surface waters have suggested the existence of alternative aerobic production pathways (Lamontagne et al. 1973; Scranton and Brewer 1977).

Recent studies have found that marine phytoplankton and cyanobacteria can produce methane aerobically (Rogers and Whitman 1991; Karl et al. 2008; Bižić et al. 2020; Klintzsch et al. 2023). Among these, *Trichodesmium*, a filamentous, colony-forming, nitrogen-fixing cyanobacterium, is particularly important due to its dominant role in nitrogen input to oligotrophic tropical and subtropical oceans (Capone et al. 1997; Bergman et al. 2013; Zehr and Capone 2020). *Trichodesmium* has been shown to use C-P lyase to degrade methylphosphonate (MPn) (Dyhrman et al. 2006), a phosphonate compound abundant in dissolved organic phosphorus pools in surface waters (Young and Ingall 2010; Repeta et al. 2016). Such utilization of MPn via cleaving the C-P bond results in methane release as a byproduct (Karl et al. 2008; White et al. 2010). Methane production in *Trichodesmium* is closely linked to its physiological state and is influenced by environmental factors including light and temperature (Zou et al. 2024). Temperature governs enzymatic activity, cellular respiration, and energy demands, often exhibiting optimal ranges for growth, nitrogen fixation, and photosynthesis in this diazotroph (Breitbarth et al. 2007; Fu et al. 2014). Light, as a fundamental driver of photosynthesis, directly regulates energy availability for its cellular processes (Küpper et al. 2004; Bell and Fu 2005; Yi et al. 2020).

Recent studies show that, under sufficient light, elevated temperatures can enhance *Trichodesmium*'s carbon and

✉ Kunshan Gao
ksgao@xmu.edu.cn

[1] State Key Laboratory of Marine Environmental Science, College of the Environment and Ecology, Xiamen University, Xiamen, China

[2] Co-Innovation Center of Jiangsu Marine Bio-Industry Technology, Jiangsu Ocean University, Lianyungang, China

Published online: 26 February 2026

nitrogen fixation as well as methane production (Zou et al. 2024). However, the dense structure of *Trichodesmium* colonies often limits light penetration, restricting photosynthesis in inner cells, as well as frequent exposure to low light in deeper waters or under cloudy weather (Carpenter and Price 1976; Prufert-Bebout et al. 1993; Eichner et al. 2019; Wang et al. 2024). Therefore, the effects of low light on methane production by *Trichodesmium* under different temperatures need to be explored. Since MPn utilization via the C-P lyase pathway is energetically costly (Kamat et al. 2011; Stasi et al. 2019), we hypothesize that light-limitation may downregulate the *Trichodesmium* C-P lyase pathway to sustain its growth, leading to non-proportional methane production in contrast to C/N assimilation. Our results show that *Trichodesmium* grown under light limitation released less methane than under optimal light conditions, leading to disrupted correlations with assimilations of carbon, nitrogen, and phosphorus.

Materials and methods

Culture conditions

Trichodesmium erythraeum IMS101 isolated from the North Atlantic Ocean, was kindly provided by Dr. David A. Hutchins (University of Southern California, Los Angeles, USA). It was grown in nitrogen-free YBCII medium (Chen et al. 1996) with the addition of 5 µM methylphosphonate (MPn; Aladdin, CAS 993–13-5, ≥ 98%). Although phosphate was not added, trace amounts of dissolved inorganic phosphorus (DIP; < 0.5 µM) were detected. The cultures were exposed to low light (30 µmol photons m^{-2} s^{-1}, white LED), which was shown as a limiting level for growth (Yi et al. 2020), and maintained at three different temperatures (23, 27, and 31 °C) on a 12-h light/dark cycle from 08:00 to 20:00 local time. Since the growth rates (doubling time ~ 11–12 days at 31 °C) were largely reduced under the low light, renewing the culture medium was done every 5–12 days, ensuring a stable range (0.005–0.025 µg mL^{-1}) of chlorophyll-*a* (Chl-*a*) concentrations parallel to other temperature regimes. Each culture was acclimated to its respective experimental conditions for at least six months (more than 15 generations) prior to data collection. Physiological and biogeochemical measurements were consistently performed at the midpoint of the dilution cycle (3–6 days post-dilution).

Chlorophyll-a concentration and growth rate

The Chl-*a* content was determined by filtering samples onto GF/F filters, extracting with 100% methanol in the dark at 4 °C overnight, and centrifuging at 12,000 × *g* for 4 min before the supernatant absorbances were measured by scanning from 250 to 800 nm. Chl-*a* was quantified as follows (Ritchie 2006):

$$Chla\left(\mu g\, mL^{-1}\right) = 12.9447 \times \left(OD_{665} - OD_{750}\right)$$

where OD_{665} and OD_{750} represent the optical densities at 665 nm and 750 nm, respectively. The specific growth rate (μ) was calculated based on changes in the concentrations of Chl-*a* in the cultures at two time points:

$$\mu\left(\text{day}^{-1}\right) = \frac{lnm_2 - lnm_1}{t_2 - t_1}$$

where m_2 and m_1 represent the Chl-*a* concentrations at time points t_1 and t_2, respectively.

Measurement of methane

Methane concentrations were accurately measured using a cavity ring-down spectrometer (Picarro G2308, USA). For each measurement, 350 mL (V_l) of sample was transferred to a polycarbonate bottle with a 270 mL headspace (V_g). The bottle was sealed with a gas-tight silicone stopper with two tubes equipped with three-way valves: one tube outlet was positioned near the liquid surface, while the other terminated in the upper headspace. The bottle was shaken to equilibrate the headspace and dissolved gases, and two gastight syringes were connected to the bottle via the three-way stopcocks. To ensure gas homogeneity, 200 mL of sterile air (C_{air}) was injected while simultaneously withdrawing 200 mL to mix with the existing headspace, resulting in a total gas volume of 470 mL during the mixing cycles. Finally, 200 mL of the headspace was used for methane determination (C_M), which was carried out every 12 h. Methane concentration in the headspace (C_g) was determined, and total methane production (bCH_4) by the culture was calculated based on the method reported previously (Johnson et al. 1990; Rao et al. 2024), accounting for the Benson solubility coefficient and temperature-specific gas constants as follows:

$$C_g = (C_M \times 470 - C_{air} \times 200)/270$$

$$b\text{CH}_4(\text{nmol day}^{-1}) = (C_{g2} - C_{g1})((\beta/22.356)RT + V_g/V_l) \times V_l/\Delta t$$

where C_{g1}, C_{g2} are headspace methane concentrations at times t_1 and t_2, respectively. β represents the Benson solubility coefficient, R the universal gas constant, and T the temperature in Kelvin.

To validate methane production specifically attributable to *Trichodesmium*, control experiments were carried out to evaluate the potential contribution of heterotrophic bacteria. In these controls, cultures were filtered through a 1.2 µm polycarbonate membrane to exclude *Trichodesmium* cells while retaining free-living bacteria. We acknowledge that

residual epibiotic bacteria attached to *Trichodesmium* trichomes may not have been completely removed. Methane production attributed to *Trichodesmium* was calculated by subtracting the methane production measured in the bacterial fraction from that of the unfiltered cultures.

Photochemical performance

Photochemical performance was assessed via fluorescence probing methods using a Multi-Color PAM fluorometer (Walz, Germany). Samples were exposed to white actinic light at growth intensity for 2 min to record steady-state fluorescence (F_s). A saturating pulse (8000 µmol photons m^{-2} s^{-1}, 0.8 s) was then applied to determine the maximum fluorescence under growth light intensity (F_m'). We measured the effective quantum yield (F_v'/F_m') without prior dark adaptation, as F_v'/F_m' can directly reflect photochemical performance of *Trichodesmium* under the experimental conditions. The effective PSII quantum yield (Fv'/Fm', Y_{II}) was determined as follows:

$$YII = (F_m' - F_s)/F_m'$$

Rapid light curves (RLCs) were measured by exposing samples to a series of light intensities ranging from 5 to 2904 µmol photons m^{-2} s^{-1} (11 steps, each lasted for 30 s). Relative electron transport rate (rETR) was calculated as (Ralph and Gademann 2005):

$$rETR = E \times YII$$

where E is the exposed light level at each step. RLC data were fitted using the model of Eilers and Peeters (1988):

$$rETR = E/(a \times E^2 + b \times e + c)$$

where the initial slope (α), representing light-use efficiency, and maximum rETR ($rETR_{max}$) were derived as:

$$\alpha = 1/c, rETR_{max} = 1/(b + 2 \times \sqrt{a \times c}).$$

Determination of assimilation rates of carbon and nitrogen

Carbon and nitrogen assimilation were quantified by measuring changes in particulate organic carbon (POC) and particulate organic nitrogen (PON) over a 24 h period (one light–dark cycle). Samples were taken at the onset of light. Cells were collected on pre-combusted (450°C, 4 h) GF/F filters and rinsed with fresh carbon- and nitrogen-free YBCII medium. The filters were then exposed to HCl fumes for 24 h to remove non-fixed inorganic carbon as CO_2. They were analyzed with an elemental analyzer (Vario EL Cube, Elementar, Germany) after having been dried. The carbon and nitrogen assimilation rates were determined by calculating the net increase in POC and PON between the onset of the light period (t = 0) and 24 h later (t = 24). The results were comparable to the POC and PON production rates assessed with POC/PON contents and specific growth rates (Tong et al. 2019; Zou et al. 2024).

Phosphorus measurements

Dissolved inorganic phosphorus (DIP) was determined for the filtrate from 0.22 µm-filtered samples using an autoanalyzer (AA3, Seal, Germany). Particulate phosphorus (PP) was analyzed via the method of Solórzano and Sharp (1980). Briefly, samples were filtered through pre-combusted GF/F filters, rinsed with 100 mL P-free BCII medium, soaked in 0.017 M $MgSO_4$, dried at 95 °C, and combusted at 450 °C for 2 h. Acid hydrolysis (0.2 M HCl, 80 °C, 30 min) converted PP to DIP, which was then quantified. Phosphorus assimilation over a diel cycle was estimated based on changes in particulate phosphorus at the onset of the light period (t = 0 h) and 24 h later (t = 24 h).

Statistical analysis

Data are presented as means ± standard deviation (n = 3, independent replicates). One-way ANOVA was employed to evaluate effects of different treatments. When significant differences were detected, Tukey's post hoc test was run to identify differences among groups. Linear regression analysis was used to examine the correlations between key variables. Data normality and homogeneity of variance were verified using the Shapiro–Wilk and Brown-Forsythe tests, respectively.

Result

Specific growth rate, Chlorophyll-a content and methane production

Temperature changes within the tested ranges significantly affected the growth of *T. erythraeum* IMS101 (Fig. 1a; one-way ANOVA, $F_{2,6} = 44.70$, $p < 0.001$). The specific growth rate was 0.18 ± 0.01 day^{-1} at 23 °C and showed no significant change at 27 °C (Tukey's test, $p = 0.714$). However, at 31 °C, growth declined sharply by 67% to 0.06 ± 0.02 day^{-1} (Tukey's test, $p < 0.001$).

Temperature also significantly influenced the relative chlorophyll-*a* content, expressed as the ratio of chlorophyll-*a* to particulate organic carbon (Chl-*a*:POC) (Fig. 1b; one-way ANOVA, $F_{2,6} = 6.25$, $p = 0.034$). As temperature increased, Chl-*a*:POC declined by 37%,

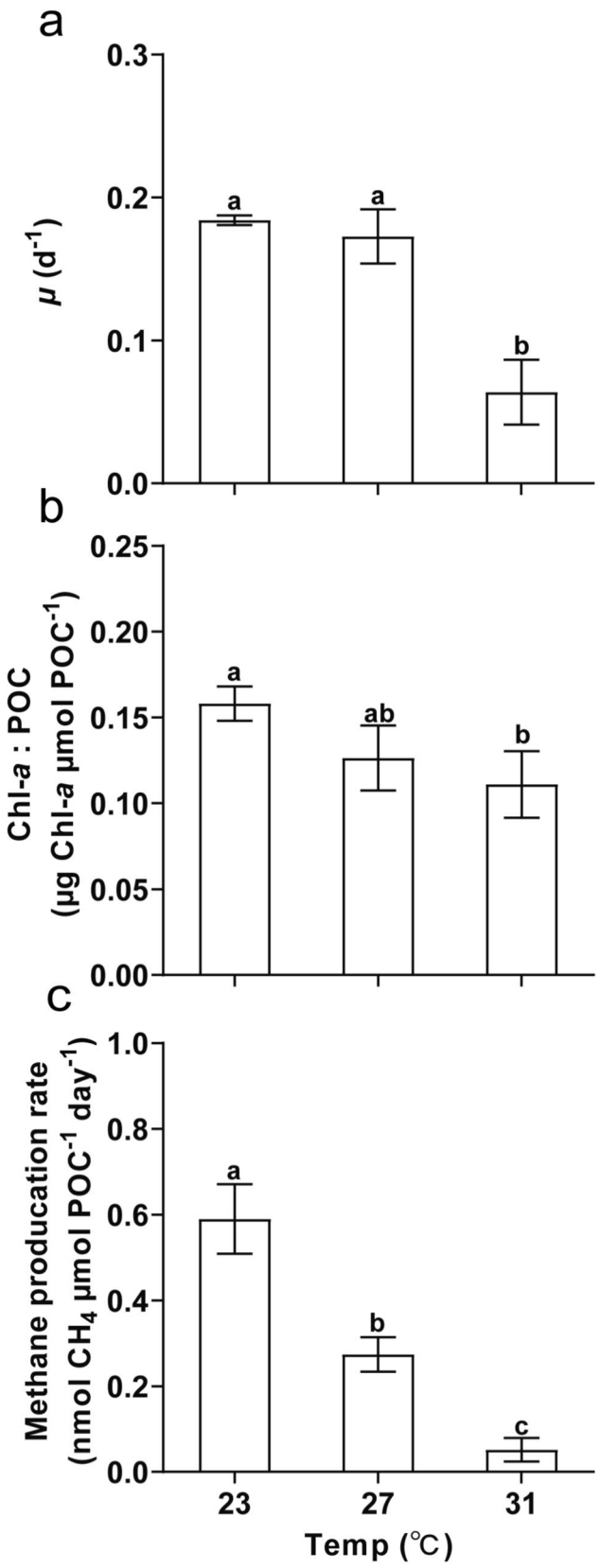

Fig. 1 Specific growth rates (**a**), chlorophyll-*a* content normalized to particulate organic carbon (Chl-*a*:POC, **b**), and methane production rates (**c**) of *Trichodesmium* after six months of acclimation to three temperatures (23, 27, and 31 °C) under low light (30 µmol photons m^{-2} s^{-1}). Data are mean ± standard deviation (SD) from three independent biological replicates (n = 3). Statistically significant differences between treatments ($p < 0.05$) are indicated by different letters

from 0.158 ± 0.010 µg Chl-*a* µmol^{-1} POC at 23 °C to 0.111 ± 0.019 µg Chl-*a* µmol^{-1} POC at 31 °C (Tukey's test, $p = 0.031$).

Methane production rate per POC declined significantly with temperature rise (Fig. 1c; one-way ANOVA, $F_{2,6} = 73.40$, $p < 0.001$). While the accumulated methane in the cultures increased over time under all treatments (Supplementary Fig. 1) till 48 h, the highest accumulation occurred at 23 °C (100 ± 12 nmol). Methane levels were markedly lower at 27 °C (35 ± 8 nmol, Tukey's test, $p = 0.009$) and 31 °C (12 ± 3 nmol, Tukey's test, $p = 0.027$). Bacterial controls produced minimal methane (3–10 nmol) at all temperatures, confirming negligible non-phototrophic contributions. The methane production rate decreased by 91%, from 0.590 ± 0.081 at 23 °C to 0.052 ± 0.028 nmol CH_4 µmol^{-1} POC day^{-1} at 31 °C (Tukey's test, $p < 0.0001$).

Photosynthetic performance

Under the growth conditions, temperature rise from 23 to 31 °C significantly influenced the effective quantum yield (YII), light utilization efficiency (α) and the maximum relative electron transport rate ($rETR_{max}$) (Fig. 2, one-way ANOVA: YII, $F_{2,6} = 10.31$, $p = 0.011$; α, $F_{2,6} = 23.70$, $p = 0.001$; $rETR_{max}$, $F_{2,6} = 60.88$, $p < 0.001$). As temperature increased from 23 °C to 31 °C, YII rose by 3% (from 0.63 ± 0.001 to 0.65 ± 0.005; Tukey's test, $p = 0.003$), α increased by 4% (from 0.68 ± 0.004 to 0.71 ± 0.010; $p = 0.012$), and $rETR_{max}$ grew by 10% (from 202 ± 2 to 222 ± 3 µmol e m^{-2} s^{-1}; $p = 0.001$).

Carbon, nitrogen and phosphorus assimilation

Under low light, temperature changes had no statistically significant effect on carbon, nitrogen and phosphorus assimilation (Fig. 3, one-way ANOVA: carbon, $F_{2,5} = 0.68$, $p = 0.550$; nitrogen, $F_{2,6} = 2.03$, $p = 0.213$; phosphorus, $F_{2,6} = 1.06$, $p = 0.404$). Specifically, carbon assimilation rates were 153 ± 14, 256 ± 174, and 204 ± 16 nmol C µmol^{-1} POC day^{-1} at 23 °C, 27 °C, and 31 °C, respectively. Nitrogen assimilation rated 40 ± 7, 41 ± 11, and 25 ± 13 nmol N µmol^{-1} POC day^{-1}, while phosphorus assimilation was 0.49 ± 0.02, 0.28 ± 0.16, and 0.32 ± 0.28 nmol P µmol^{-1} POC day^{-1} at the corresponding three temperature levels. Furthermore, linear regression analysis showed no significant relationship between methane production and the assimilation of

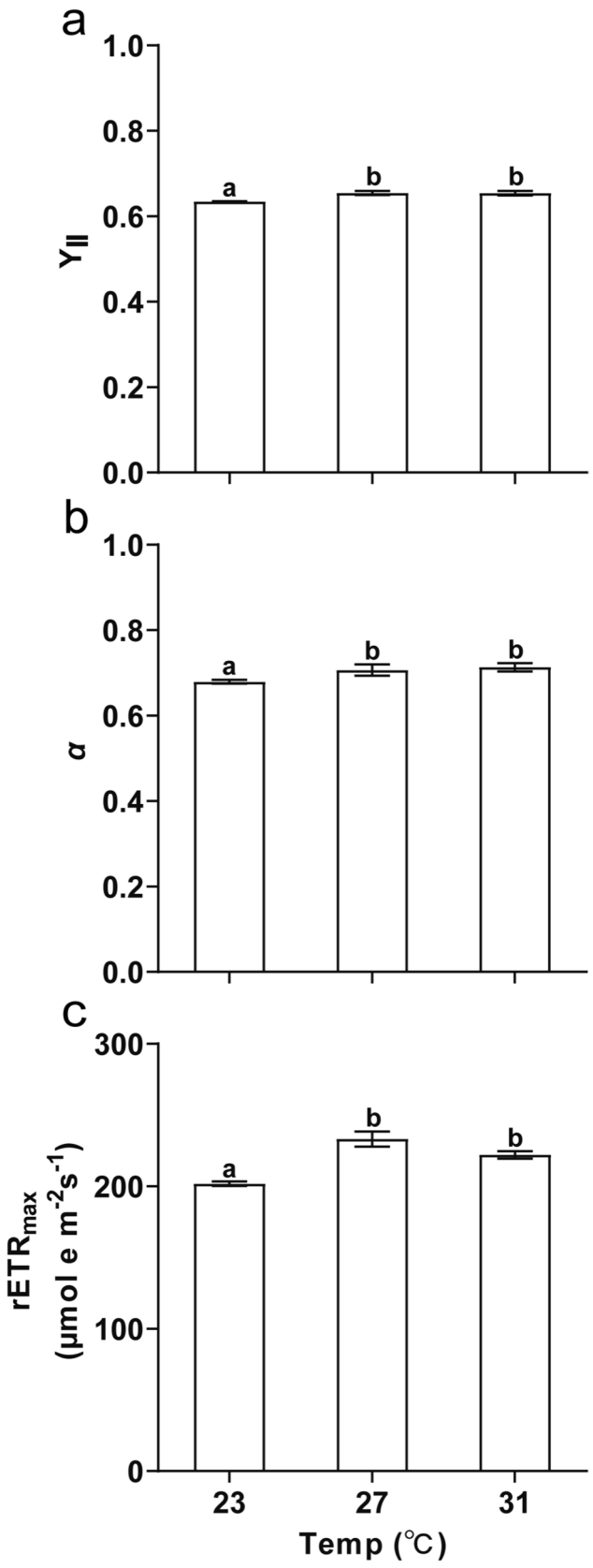

Fig. 2 Photosynthetic parameters of *Trichodesmium* after long-term acclimation to varying temperature conditions under low light (30 μmol photons m^{-2} s^{-1}). Parameters include (**a**) effective quantum yield (YII), (**b**) initial slope of the rapid light curve (α, indicating light utilization efficiency), and (**c**) maximum relative electron transport rate ($rETR_{max}$). The α and rETR, were derived from the rapid light curves (Supplementary Fig. S2). Data are presented as means ± SD (n = 3), with different letters indicating statistically significant differences ($p < 0.05$)

carbon ($F_{1,6} = 0.28$, $p = 0.613$, $R^2 = 0.045$, Fig. 4), nitrogen ($F_{1,6} = 3.69$, $p = 0.103$, $R^2 = 0.381$), or phosphorus ($F_{1,7} = 1.7$, $p = 0.248$, $R^2 = 0.185$). The methane production quotients (MPQ), defined as the ratio of carbon or nitrogen assimilation to methane production rates, varied with temperature. Specifically, MPQ values for carbon were 258, 937, and 3949; and for nitrogen were 67, 151, and 490, at 23 °C, 27 °C, and 31 °C, respectively.

Discussion

Our results reveal a distinct decoupling between methane production and carbon/nitrogen assimilation in *Trichodesmium* grown under light-limited conditions (30 μmol photons m^{-2} s^{-1}), particularly at 31 °C (Fig. 4). This contrasts with our previous finding under optimal light, where methane release scaled linearly with carbon and nitrogen fixation (Zou et al. 2024). These contrasting findings underscore the high energetic cost of methylphosphonate (MPn) utilization. The C-P lyase pathway involves PhnCDE-mediated transport and reductive bond cleavage, processes that demand significant ATP and reducing power (e.g., NADPH) (Kamat et al. 2011; Stasi et al. 2019). Consequently, under light limitation, the restricted supply of photosynthetic energy cannot meet the energetic demands of C-P cleavage, thereby uncoupling methane production from carbon and nitrogen fixation.

Under moderate light conditions, representative of 20-40 m depths in waters where *Trichodesmium* thrives (Capone et al. 1997; Piazena et al. 2002), rising temperatures have been shown to enhance nitrogen fixation, photosynthetic rates and growth (Breitbarth et al. 2007; Hutchins et al. 2007; Levitan et al. 2010; Boatman et al. 2017; Jiang et al. 2018; Yi et al. 2020). Methane production under these conditions also increases with temperature rise, with the maximal ratios of carbon and nitrogen fixation to methane production ranging from 227 to 494 and 40 to 128, respectively (Zou et al. 2024). However, at low light (30 μmol photons m^{-2} s^{-1}), approximating 60–80 m depths (Piazena et al. 2002), when the temperature was raised from 23 to 31 °C, growth and methane production were reduced remarkably (Fig. 1). This indicates that degradation and subsequent utilization of MPn is energy-limited at this light intensity.

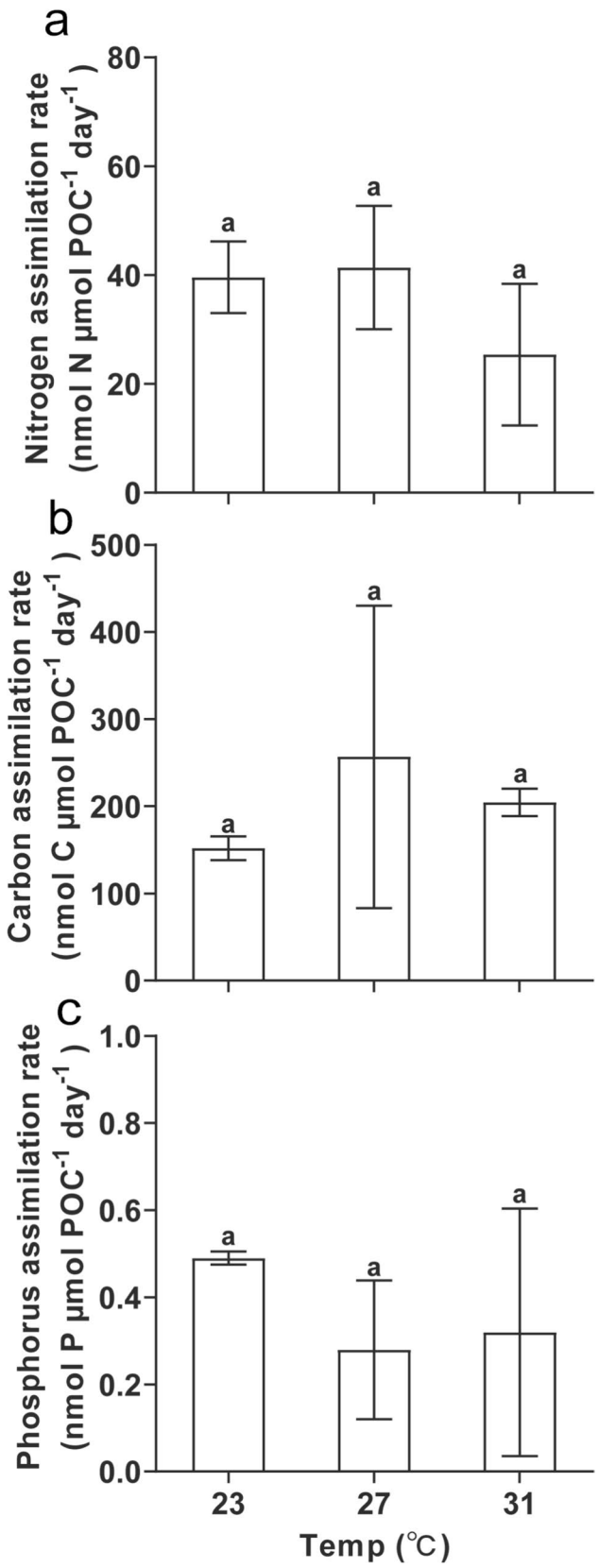

Fig. 3 Assimilation rates of carbon (**a**), nitrogen (**b**), and phosphorus (**c**) in *Trichodesmium* under low light (30 µmol photons m^{-2} s^{-1}) at three acclimation temperatures (23, 27, and 31 °C). Data are mean ± SD of three independent biological replicates. Statistically significant differences are highlighted by distinct letters ($p < 0.05$)

Interestingly, this energy limitation was not evident at the lower temperature of 23 °C. Under this condition, the methane production rates were comparable between the light-limited (0.59 ± 0.08 nmol CH_4 µmol^{-1} POC day^{-1}) and optimal-light (0.46 ± 0.05 nmol CH_4 µmol^{-1} POC day^{-1}) conditions (Supplementary Table 1). This suggests that at 23 °C, reduced enzymatic activity was the primary limiting factor controlling metabolic rates. Reduced temperature lowers overall enzymatic turnover and metabolic energy demand (Davison 1991; Peterson et al. 2007). Furthermore, *Trichodesmium* effectively compensated for low light by upregulating its chlorophyll-*a* content by about 100% compared to the optimal light level (Zou et al. 2024). Consequently, at 23 °C, physiological acclimation was sufficient to sustain MPn utilization even under low light.

However, this delicate balance collapses when the temperature rises to 31 °C. Increased temperature enhances respiration, which consumes a larger fraction of the energy pool and organic matter (Raven and Geider 1988; Boatman et al. 2017), leaving insufficient ATP to sustain the energetically costly C-P lyase pathway (Kamat et al. 2011; Stasi et al. 2019). Crucially, thermal stress at 31 °C likely drives an alternative P-acquisition strategy: enhanced phosphorus turnover via the remineralization of dissolved organic phosphorus (DOP), particularly phosphate esters (Sohm and Capone 2006; Piontek et al. 2009). Given that the C-O-P bonds in these esters are more labile and bioavailable compared to stable C-P bonds (Dyhrman et al. 2006; Beversdorf et al. 2010), light-limited cells likely shift their preference toward these remineralized P sources. This metabolic switch reduces the reliance on MPn, providing a robust explanation for why methane production drops sharply even while cellular P assimilation is maintained (Fig. 1, 3).

As ocean temperatures continue to rise under progressive climate change (Collins et al. 2013), the interaction between light and temperature is expected to play a crucial role in shaping oceanic methane emissions. Our previous work (Zou et al. 2024) demonstrated that warming above 27 °C may enhance *Trichodesmium*'s MPn-dependent methane production, implying that, as long as the photosynthetic energy supply is sufficient, increased enzyme activities with warming can raise the ratios of methane released to C or N fixed (Somavilla et al. 2017; Frischkorn et al. 2018; Ulloa et al. 2019). Based on the results from this work, however, the warming effect might be mitigated if *Trichodesmium* colonies sink to deeper light-limited

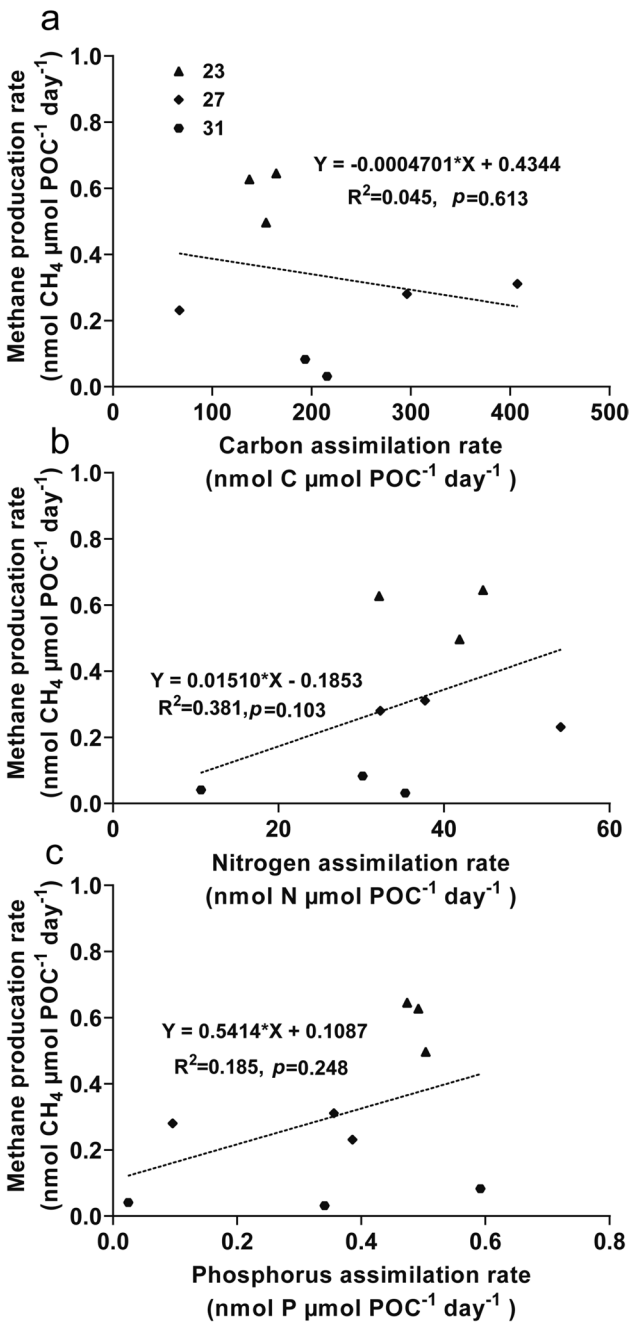

Fig. 4 Correlations between methane production rates and assimilation rates of carbon (**a**), nitrogen (**b**), and phosphorus (**c**) in *Trichodesmium*. Data were compiled from Figs. 1 and 3. Different symbols with numbers represent the corresponding growth temperatures (°C). Each point represents an individual biological replicate

layers to access nutrients, where insufficient light limits methane production (Villareal and Carpenter 1990; Eichner et al. 2023).

Supplementary Information The online version contains supplementary material available at https://doi.org/10.1007/s10811-026-03815-x.

Acknowledgements The authors are grateful to the laboratory engineers Xianglan Zeng and Wenyan Zhao for their technical and logistical supports.

Authors contribution KG and CZ conceived and designed the experiment. CZ performed the experiments and analyses. CZ, and KG analyzed the data and contributed to the writing and editing of the manuscript.

Funding This study was supported by National Natural Science Foundation of China (No. 42361144840 and 41720104005) to KG, 42506094 to CZ.

Data availability The data are available by request from the corresponding author.

Declarations

Competing interests The authors declare no competing interests.

References

Bell PRF, Fu F-X (2005) Effect of light on growth, pigmentation and N_2 fixation of cultured *Trichodesmium* sp. from the Great Barrier Reef lagoon. Hydrobiologia 543:25–35

Bergman B, Sandh G, Lin S, Larsson J, Carpenter EJ (2013) *Trichodesmium* - a widespread marine cyanobacterium with unusual nitrogen fixation properties. FEMS Microbiol Rev 37:286–302

Beversdorf LJ, White AE, Björkman KM, Letelier RM, Karl DM (2010) Phosphonate metabolism by *Trichodesmium* IMS101 and the production of greenhouse gases. Limnol Oceanogr 55:1768–1778

Bižić M, Klintzsch T, Ionescu D, Hindiyeh M, Günthel M, Muro-Pastor AM, Eckert W, Urich T, Keppler F, Grossart H-P (2020) Aquatic and terrestrial cyanobacteria produce methane. Sci Adv 6:eaax5343

Boatman TG, Lawson T, Geider RJ (2017) A key marine diazotroph in a changing ocean: the interacting effects of temperature, CO_2 and light on the growth of *Trichodesmium erythraeum* IMS101. PLoS ONE 12:e0168796

Breitbarth E, Oschlies A, LaRoche J (2007) Physiological constraints on the global distribution of *Trichodesmium*–effect of temperature on diazotrophy. Biogeosciences 4:53–61

Capone DG, Zehr JP, Paerl HW, Bergman B, Carpenter EJ (1997) *Trichodesmium*, a globally significant marine cyanobacterium. Science 276:1221–1229

Carpenter EJ, Price CC (1976) Marine *Oscillatoria* (*Trichodesmium*): explanation for aerobic nitrogen fixation without heterocysts. Science 191:1278–1280

Chen YB, Zehr JP, Mellon M (1996) Growth and nitrogen fixation of the diazotrophic filamentous nonheterocystous cyanobacterium *Trichodesmium* sp. IMS 101 in defined media: evidence for a circadian rhythm. J Phycol 32:916–923

Collins M, Knutti R, Arblaster J, Dufresne J-L, Fichefet T, Friedlingstein P, Gao X, Gutowski WJ, Johns T, Krinner G (2013) Long-term climate change: projections, commitments and irreversibility. In: Climate Change 2013: The Physical Science Basis. IPCC Working Group I Contribution to AR5 (Eds). IPCC, Cambridge University Press. Cambridge, pp 1029–1136

Davison IR (1991) Environmental effects on algal photosynthesis: temperature. J Phycol 27:2–8

Dyhrman ST, Chappell PD, Haley ST, Moffett JW, Orchard ED, Waterbury JB, Webb EA (2006) Phosphonate utilization by the globally important marine diazotroph *Trichodesmium*. Nature 439:68–71

Eichner M, Inomura K, Pierella Karlusich JJ, Shaked Y (2023) Better together? Lessons on sociality from *Trichodesmium*. Trends Microbiol 31:1072–1084

Eichner M, Thoms S, Rost B, Mohr W, Ahmerkamp S, Ploug H, Kuypers MMM, de Beer D (2019) N_2 fixation in free-floating filaments of *Trichodesmium* is higher than in transiently suboxic colony microenvironments. New Phytol 222:852–863

Eilers P, Peeters J (1988) A model for the relationship between light intensity and the rate of photosynthesis in phytoplankton. Ecol Model 42:199–215

Frischkorn KR, Krupke A, Guieu C, Louis J, Rouco M, Salazar Estrada AE, Van Mooy BA, Dyhrman ST (2018) *Trichodesmium* physiological ecology and phosphate reduction in the western tropical South Pacific. Biogeosciences 15:5761–5778

Fu F-X, Yu E, Garcia NS, Gale J, Luo Y, Webb EA, Hutchins DA (2014) Differing responses of marine N_2 fixers to warming and consequences for future diazotroph community structure. Aquat Microb Ecol 72:33–46

Hutchins DA, Fu F-X, Zhang Y, Warner ME, Feng Y, Portune K, Bernhardt PW, Mulholland MR (2007) CO_2 control of *Trichodesmium* N_2 fixation, photosynthesis, growth rates, and elemental ratios: implications for past, present, and future ocean biogeochemistry. Limnol Oceanogr 52:1293–1304

IPCC (2013) Climate change 2013 – the physical science basis: working group I contribution to the fifth assessment report of the Intergovernmental Panel on Climate Change. Cambridge University Press, Cambridge. https://doi.org/10.1017/CBO9781107415324

Jiang H-B, Fu F-X, Rivero-Calle S, Levine NM, Sañudo-Wilhelmy SA, Qu P-P, Wang X-W, Pinedo-Gonzalez P, Zhu Z, Hutchins DA (2018) Ocean warming alleviates iron limitation of marine nitrogen fixation. Nat Clim Change 8:709–712

Johnson KM, Hughes JE, Donaghay PL, Sieburth JM (1990) Bottle-calibration static head space method for the determination of methane dissolved in seawater. Anal Chem 62:2408–2412

Kamat SS, Williams HJ, Raushel FM (2011) Intermediates in the transformation of phosphonates to phosphate by bacteria. Nature 480:570–573

Karl DM, Beversdorf L, Björkman KM, Church MJ, Martinez A, Delong EF (2008) Aerobic production of methane in the sea. Nat Geosci 1:473–478

Karl DM, Tilbrook BD (1994) Production and transport of methane in oceanic particulate organic matter. Nature 368:732–734

Klintzsch T, Geisinger H, Wieland A, Langer G, Nehrke G, Bizic M, Greule M, Lenhart K, Borsch C, Schroll M (2023) Stable carbon isotope signature of methane released from phytoplankton. Geophys Res Lett 50:e2023GL103317

Küpper H, Ferimazova N, Setlík I, Berman-Frank I (2004) Traffic lights in *Trichodesmium*. Regulation of photosynthesis for nitrogen fixation studied by chlorophyll fluorescence kinetic microscopy. Plant Physiol 135:2120–2133

Lamontagne R, Swinnerton J, Linnenbom V, Smith W (1973) Methane concentrations in various marine environments. J Geophys Res 78:5317–5324

Levitan O, Brown CM, Sudhaus S, Campbell D, LaRoche J, Berman-Frank I (2010) Regulation of nitrogen metabolism in the marine diazotroph *Trichodesmium* IMS101 under varying temperatures and atmospheric CO_2 concentrations. Environ Microbiol 12:1899–1912

Peterson ME, Daniel RM, Danson MJ, Eisenthal R (2007) The dependence of enzyme activity on temperature: determination and validation of parameters. Biochem J 402:331–337

Piazena H, Perez-Rodrigues E, Häder D-P, Lopez-Figueroa F (2002) Penetration of solar radiation into the water column of the central subtropical Atlantic Ocean—optical properties and possible biological consequences. Deep Sea Res II 49:3513–3528

Piontek J, Händel N, Langer G, Wohlers J, Riebesell U, Engel A (2009) Effects of rising temperature on the formation and microbial degradation of marine diatom aggregates. Aquat Microb Ecol 54:305–318

Prufert-Bebout L, Paerl HW, Lassen C (1993) Growth, nitrogen fixation, and spectral attenuation in cultivated *Trichodesmium* species. Appl Environ Microbiol 59:1367–1375

Ralph PJ, Gademann R (2005) Rapid light curves: a powerful tool to assess photosynthetic activity. Aquat Bot 82:222–237

Rao Y, Gao G, Berman-Frank I, Bizic M, Gao K (2024) Light-dependent methane production by a coccolithophorid may counteract its photosynthetic contribution to carbon dioxide sequestration. Commun Earth Environ 5:695

Raven JA, Geider RJ (1988) Temperature and algal growth. New Phytol 110:441–461

Repeta DJ, Ferrón S, Sosa OA, Johnson CG, Repeta LD, Acker M, Delong EF, Karl DM (2016) Marine methane paradox explained by bacterial degradation of dissolved organic matter. Nat Geosci 9:884–887

Ritchie RJ (2006) Consistent sets of spectrophotometric chlorophyll equations for acetone, methanol and ethanol solvents. Photosynth Res 89:27–41

Rogers JE, Whitman WB (1991) Microbial production and consumption of greenhouse gases: methane, nitrogen oxides, and halomethanes. American Society for Microbiology, Washington

Saunois M, Stavert AR, Poulter B, Bousquet P, Canadell JG et al (2020) The global methane budget 2000–2017. Earth Syst Sci Data 12:1561–1623

Scranton MI, Brewer PG (1977) Occurrence of methane in the near-surface waters of the western subtropical North-Atlantic. Deep Sea Res 24:127–138

Sohm JA, Capone DG (2006) Phosphorus dynamics of the tropical and subtropical north Atlantic: *Trichodesmium* spp. versus bulk plankton. Mar Ecol Prog Ser 317:21–28

Solórzano L, Sharp JH (1980) Determination of total dissolved phosphorus and particulate phosphorus in natural waters. Limnol Oceanogr 25:754–758

Somavilla R, González-Pola C, Fernández-Diaz J (2017) The warmer the ocean surface, the shallower the mixed layer. How much of this is true? J Geophys Res Oceans 122:7698–7716

Stasi R, Neves HI, Spira B (2019) Phosphate uptake by the phosphonate transport system PhnCDE. BMC Microbiol 19:79

Tong S, Hutchins DA, Gao K (2019) Physiological and biochemical responses of *Emiliania huxleyi* to ocean acidification and warming are modulated by UV radiation. Biogeosciences 16:561–572

Ulloa HN, Winters KB, Wüest A, Bouffard D (2019) Differential heating drives downslope flows that accelerate mixed-layer warming in ice-covered waters. Geophys Res Lett 46:13872–13882

Villareal TA, Carpenter EJ (1990) Diel buoyancy regulation in the marine diazotrophic cyanobacterium *Trichodesmium thiebautii*. Limnol Oceanogr 35:1832–1837

Wang S, Zhang F, Koedooder C, Qafoku O, Basu S, Krisch S, Visser AN, Eichner M, Kessler N, Boiteau RM (2024) Costs of dust collection by *Trichodesmium*: effect on buoyancy and toxic metal release. J Geophys Res Biogeosci 129:e2023JG007954

White AE, Karl DM, Björkman KM, Beversdorf LJ, Letelier RM (2010) Production of organic matter by *Trichodesmium IMS101* as a function of phosphorus source. Limnol Oceanogr 55:1755–1767

Yi X, Fu F-X, Hutchins DA, Gao K (2020) Light availability modulates the effects of warming in a marine N_2 fixer. Biogeosciences 17:1169–1180

Young CL, Ingall ED (2010) Marine dissolved organic phosphorus composition: insights from samples recovered using combined electrodialysis/reverse osmosis. Aquat Geochem 16:563–574

Zehr JP, Capone DG (2020) Changing perspectives in marine nitrogen fixation. Science 368:eaay9514

Zou C, Yi X, Li H, Bizic M, Berman-Frank I, Gao K (2024) Correlation of methane production with physiological traits in *Trichodesmium* IMS 101 grown with methylphosphonate at different temperatures. Front Microbiol 15:1396369